Semicond. Sci. Technol. **22** (2007) 963–969 doi:10.1088/0268-1242/22/8/023

Analysis of generation and annihilation of deep level defects in a silicon-irradiated bipolar junction transistor

K V Madhu[1], S R Kulkarni[2], M Ravindra[3] and R Damle[1]

[1] Department of Physics, Jnanabharati, Bangalore University, Bangalore 560 056, India
[2] Department of Physics, Center for PG Studies, SBMJC, Jayanagar, Bangalore 560 011, India
[3] Components Division, ICG, ISRO Satellite Centre, Airport Road, Bangalore 560 017, India

E-mail: damleraju@yahoo.com

Received 12 March 2007, in final form 5 May 2007
Published 19 July 2007
Online at stacks.iop.org/SST/22/963

Abstract

A commercial bipolar junction transistor (2 N 2219 A, npn), irradiated with 120 MeV Si^{9+} ions with a fluence of the order of 10^{12} ions cm^{-2}, is studied for radiation-induced gain degradation and deep level defects. *I–V* measurements are made to study the gain degradation as a function of ion fluence. Properties such as activation energy, trap concentration and capture cross section of deep levels are studied by deep level transient spectroscopy (DLTS). Minority carrier trap energy levels with energies ranging from $E_C - 0.160$ eV to $E_C - 0.581$ eV are observed in the base-collector junction of the transistor. Majority carrier trap levels are also observed with energies ranging from $E_V + 0.182$ eV to $E_V + 0.401$ eV. The identification of the defect type is made on the basis of its finger prints such as activation energy, annealing temperature and capture cross section by comparing with those reported in the literature. New energy levels for the defects A-center, di-vacancy and Si-interstitial are also observed. The irradiated transistor is subjected to isothermal and isochronal annealing. The defects are seen to anneal above 250 °C. The defects generated in the base region of the transistor by displacement damage appear to be responsible for transistor gain degradation.

1. Introduction

Bipolar junction transistors (BJTs) are still being extensively used in space and other radiation-rich environments. These devices are sensitive to high energy particle irradiation. A considerable amount of data is available on the radiation effects of γ-rays, fast neutrons, electrons and protons on semiconductor devices [1–5]. However, there appears to be rather little work on heavy ion-induced effects and consequent characterization of defects by the deep level transient spectroscopy (DLTS) technique. Deep level defect monitoring plays an important role in designing a semiconductor device suitably for various applications. A study of radiation-induced effects in semiconductor devices is thus important not only to observe changes in electrical characteristics, but also to get the basic information regarding the generation and annihilation of defects.

Exposure of semiconductor devices to high energy particle radiation is known to generate a variety of defects. The nature of these defects generated by irradiation process depends on the properties of target as well as impinging high energy particle. To investigate these deep level defects, several techniques are in practice. DLTS is now an established technique for detecting and characterizing a variety of defects in semiconductor devices. DLTS is a high frequency capacitance transient thermal scanning method useful for observing a wide variety of traps in semiconductor devices [6]. This technique is capable of displaying the spectrum of traps in a crystal as positive and negative peaks on a flat base line as a function of temperature. From the analysis of the DLTS spectrum, one can measure the activation energy, concentration profile and capture cross section of the defects observed.

In the present work, the radiation response of a BJT (2 N 2219 A, npn) designed for space applications is studied. *I–V* measurements as a function of Si^{9+} ion fluence as well as DLTS studies are made to gather an insight into the mechanism of transistor gain degradation. The BJT used in the present study has been thoroughly studied in our earlier work for 24 MeV protons, 8 MeV electrons and ^{60}Co γ-rays-induced effects [7–9]. A DLTS study of deep level defects in Li-ion-irradiated transistor (chosen from the same batch) is also reported earlier [10].

2. Experimental details

A commercial BJT (2 N 2219 A, npn) manufactured in an indigenous technology from Continental Device India Ltd. (CDIL) has been selected for the present study. This device is a switching transistor with standard configuration (base thickness is 2.0 μm and oxide thickness is 1.2 μm) suitable for low and high frequency operation. A decapped transistor is exposed to 120 MeV Si^{9+} ions using 15 UD 16 MV pelletron Tandem Van de Graff accelerator facility at the Inter-University Accelerator Centre, New Delhi. The transistor under the biased condition (CE mode) is irradiated by Si^{9+} ions with two different fluences 9.4×10^{11} ions cm^{-2} and 3.1×10^{12} ions cm^{-2}. During irradiation, the target chamber is maintained at room temperature (300 K) and low pressure (7.5×10^{-9} Torr). The ion fluences are calculated by measuring the ion beam current and irradiation time. The ion beam current is fixed at 1 pnA (particle nanoampere, 1 pnA = (6.25×10^9) /(charge state of the ion)), ion fluence = beam current in pnA × irradiation time in seconds. A Keithley 236 source meter interfaced to a computer is used for *I–V* measurements. Output characteristics of the transistor are studied at a constant base current (I_B) of 50 μA. The collector voltage (V_{CE}) is varied from −0.1 V to 2.5 V in the steps of 0.01 V. Gummel plots are acquired by varying base emitter voltage (V_{BE}) from 0 V to 0.7 V in the steps of 0.01 V at a constant collector voltage (V_{CE}) of 5 V.

DLTS spectra are recorded for both unirradiated transistor and two different transistors of the same batch (date code) exposed to the Si^{9+} ion for two different fluences. The DLTS system (IMS-2000, M/s. Lab Equip, India) employed for the present study consists of a boxcar averager, a pulse generator, a thousand point digitizer, a voltage generator and a high speed capacitance meter. The pulse generator is capable of generating pulses of widths ranging from 100 ns to 10 s. The pulse height could be programmed from −12 V to +12 V. The boxcar averager is capable of generating seven rate windows. The time constants can be varied from 1 ms to 2 s. In the present study, a reverse bias of 4 V is applied to the collector-base junction of the transistor. The filling bias voltage or pulse height is fixed at 0 V and the pulse width is fixed at 19.2 ms. DLTS signals corresponding to seven rate windows are obtained enabling construction of Arrhenius plots from a single temperature scan and are fixed at 1.3, 3.3, 8.3, 20.8, 51.7, 127.9 and 312.7 s^{-1}. The trap concentration, activation energy and capture cross section of different deep levels are determined by DLTS spectra.

The silicon-ion-irradiated bipolar junction transistors are subjected to isothermal and isochronal (30 min) annealing.

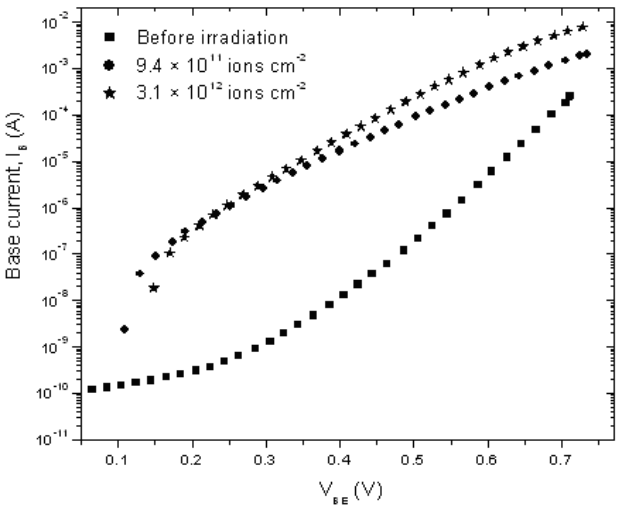

Figure 1. Variation of I_B with V_{BE} for two different ion fluences (at constant $V_{CE} = 5$ V).

The annealing temperature in the furnace can be maintained constant for several hours with an accuracy of 1 °C. During isochronal (30 min) annealing, the temperature is varied from 100 °C to 450 °C. During isothermal (100 °C) annealing, the annealing time is varied from 30 min to 480 min. DLTS spectra are recorded at different stages of thermal annealing and the characteristics of several deep level defects are monitored.

3. Results and discussion

3.1. I–V measurements

In general, any disturbance of lattice periodicity in the bulk of the semiconductor may give rise to energy levels in the band gap. Radiation-induced defects may have such energy levels with them that these defects can have a major impact on the electrical characteristics of the transistor [11]. Figures 1 and 2 exhibit Gummel plots (variation of the base current I_B, collector current I_C with the base voltage V_{BE}) before and after irradiation by Si^{9+} ions. It is observed that the base current increases with ion fluence. However, the collector current decreases as the ion fluence increases.

One important aspect of characterization of BJTs for radiation-induced effects is radiation-induced gain degradation. The BJTs are particularly found to be vulnerable to ionizing radiation, and the transistor gain degradation is the primary cause for parametric shifts and functional failures. The degradation of forward current gain of BJT when exposed to radiation is dependent on many factors including the nature of radiation particulate and dose rate. It is well known that the transistor gain degradation can occur due to the generation of recombination centers in the base region due to displacement damage caused upon irradiation. When recombination centers are generated in the base region of the transistor, it leads to an increase in the base current by decreasing the minority carrier lifetime [12, 13]. A decrease in the minority carrier lifetime will be reflected in the degradation of forward current gain of the transistor.

Figure 3 shows the collector characteristics of the transistor irradiated with 3.1×10^{12} ions cm^{-2} at different

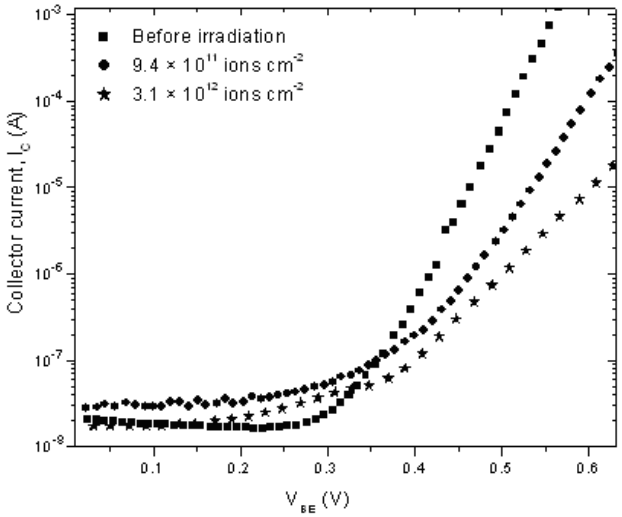

Figure 2. Variation of I_C with V_{BE} for two different ion fluences (at constant $V_{CE} = 5$ V).

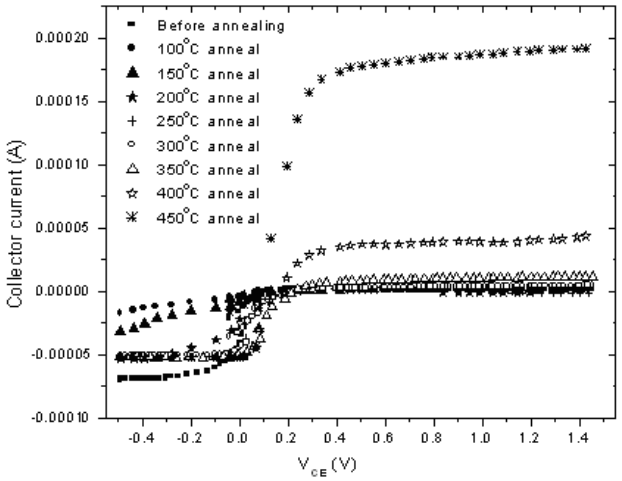

Figure 3. Collector characteristics of the transistor at different isochronal (30 min) annealing temperatures (at constant $I_B = 50$ μA).

isochronal (30 min) annealing temperatures. The isochronal annealing clearly shows that there is a major recovery in the collector current above 400 °C. Figure 4 exhibits the variation of I_B and I_C as a function of annealing temperature. It is found that while collector current increases with an increase in the annealing temperature, the base current decreases.

3.2. C–V measurements

Figure 5 shows the capacitance–voltage (C–V) characteristics of the base-collector junction of the transistor before and after irradiation. The plot shows that there is a considerable degradation in the C–V characteristics of the transistor after irradiation. This would indicate that there is a partial loss of charge carriers in the base-collector junction of the transistor upon irradiation. A plot of $(1/C^2)$ versus voltage (shown in the inset) shows that the doping concentration of the base-collector junction of the transistor increases from 2.4×10^{13} cm^{-3} to 1.7×10^{14} cm^{-3} upon Si^{9+} ion irradiation. Figure 6

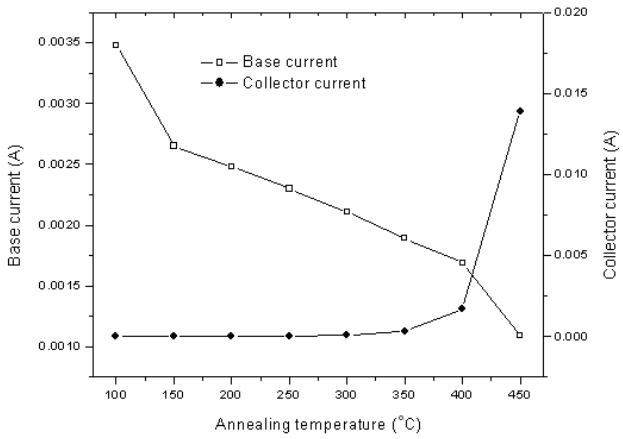

Figure 4. Variation of I_B and I_C as a function of isochronal (30 min) annealing temperature (at constant $V_{BE} = 0.55$ V).

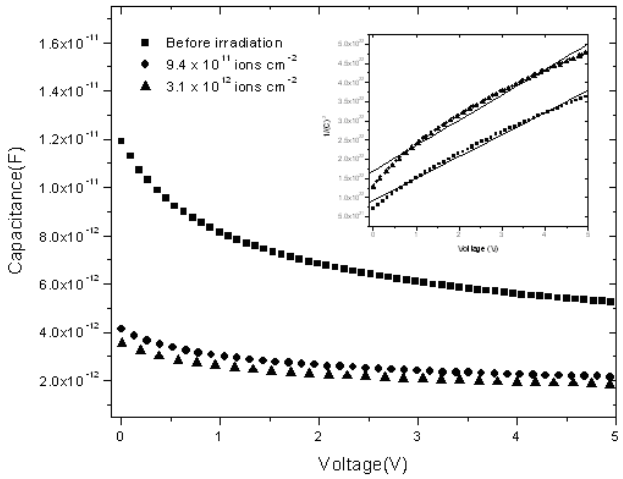

Figure 5. Capacitance–voltage characteristics of the base-collector junction of the transistor for two different ion fluences.

shows the C–V characteristics of the base-collector junction of the transistor irradiated with 3.1×10^{12} ions cm^{-2} at different isochronal (30 min) annealing temperatures. The C–V characteristics appear to improve after the temperature 300 °C.

3.3. DLTS measurements

In principle, irradiation by any ion can damage transistors through both ionization and displacement. Ionization is a surface phenomenon. Displacement damage is a bulk phenomenon which results in the generation of several types of defects such as vacancy, interstitial, di-vacancy, Frenkel pair, vacancy-impurity complexes namely A-center (V-O), E-center (V-P), boron–carbon interstitial clusters and di-interstitial or higher order complexes called D-center [11–14].

The concept of nonionizing energy loss (NIEL) has been found useful for characterizing displacement damage effects in materials and devices [15–19]. NIEL is the rate of energy loss due to atomic displacements as an incident ion traverses the material. The product of the NIEL (MeV cm^2 g^{-1}) and the particle fluence (ions cm^{-2}) gives the displacement damage

Table 1. Displacement damage dose data for 120 MeV Si ion in a silicon target for two different ion fluences.

Ion fluence (ions cm^{-2})	Vacancy production rate (vacancies ion^{-1} cm^{-1})		Total displacements (cm^{-2})	NIEL (MeV cm^2 g^{-1})	Displacement damage dose (rad)
	Due to ions	Due to recoils			
9.4×10^{11}	2.9×10^5	2.4×10^4	4.5×10^{14}	6.95	1.04×10^5
3.1×10^{12}			1.4×10^{15}		3.40×10^5

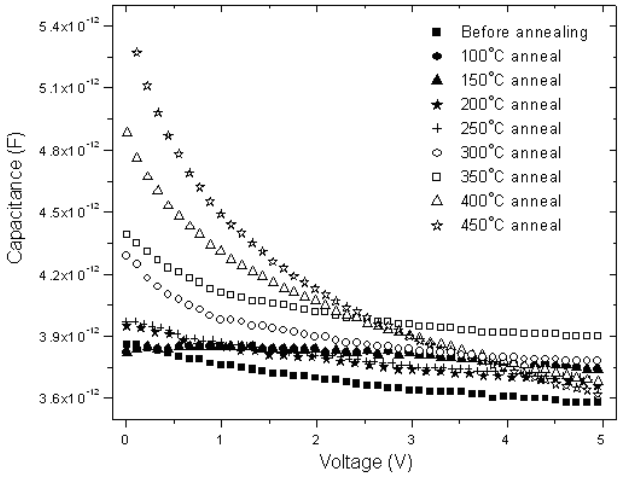

Figure 6. Capacitance–voltage characteristics of the base-collector junction of the transistor at different isochronal (30 min) annealing temperatures.

dose (in rad) [18, 20]. NIEL for a given ion in a target can be calculated by using SRIM program [21]. Displacement damage dose for 120 MeV Si^{9+} ion in a silicon target for two different fluences are calculated and tabulated in table 1.

The deep level defects generated by irradiation of transistors by Si^{9+} ions are characterized using the DLTS technique. The DLTS spectrum is a plot of difference in capacitance (δC) versus temperature. Figure 7 exhibits the DLTS spectra of Si^{9+}-ion-irradiated transistor for two different ion fluences. The trap concentration (N_T) can be determined by knowing the peak height (δC_{max}) in the DLTS spectrum. Activation energy (ΔE) and capture cross section (σ) of the deep levels are calculated by using the equation

$$\tau T^2 = \frac{\exp[(\Delta E)/kT]}{\gamma\sigma}. \tag{1}$$

In equation (1), γ is the material coefficient and all other symbols have a usual meaning [22]. A plot of $\ln(\tau T^2)$ versus $1/T$ is known as the Arrhenius plot; the activation energy ΔE is obtained from the slope of the plot and the capture cross section is obtained by extrapolating the plot on the Y-axis. Figure 8 exhibits the Arrhenius plots of deep level defects for two different ion fluences. Three minority carrier and two majority carrier deep level defects are observed in the DLTS spectra of the Si^{9+}-ion-irradiated transistor with an ion fluence of 9.4×10^{11} ions cm^{-2}. For the ion fluence of 3.1×10^{12} ions cm^{-2}, five minority carrier and two majority carrier defect levels are observed. The trap concentration, capture cross section and introduction rate of all the deep level defects are calculated from the DLTS spectra and presented in table 2. The activation energy of all the defects has been measured to an accuracy of 0.001 eV.

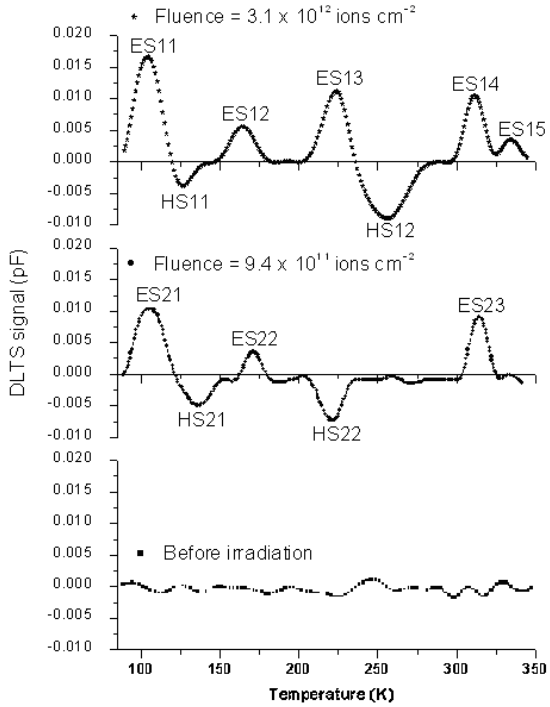

Figure 7. DLTS spectra of Si^{9+}-ion-irradiated transistor for two different ion fluences. The rate window is fixed at 312.7 s^{-1}.

A recombination of electron–hole pairs at the defect levels generated upon displacement damage is the most important physical phenomenon responsible for the gain degradation. Mainly, four kinds of recombination processes are observed in semiconductor devices: (i) Shockley–Read–Hall (SRH) or multi-phonon recombination, (ii) radiative recombination, (iii) Auger recombination and (iv) non-radiative recombination [22]. Radiative recombination is important in direct band gap semiconductors like GaAs. Auger recombination is observed in either direct or indirect band gap semiconductors when the carrier concentration is high. Further, the radiative, non-radiative and Auger recombination lifetimes are independent of trap concentration [22]. SRH recombination is particularly important in indirect band gap semiconductors such as Si [23–27]. SRH recombination lifetime (for low level injection) is calculated using the equation

$$\tau_{SRH} = \frac{1}{\sigma_n v_{th} N_T}. \tag{2}$$

In equation (2), σ_n is the minority carrier capture cross section, v_{th} is the thermal velocity of the carriers and N_T is the total trap concentration. Similarly, the radiative recombination lifetime is given by

$$\tau_{rad} = [B(p_0 + n_0 + \Delta n)]^{-1}. \tag{3}$$

Table 2. Data obtained from the DLTS analysis of the irradiated transistor.

Ion fluence (ions cm^{-2})	Defect label	Defect type	Activation energy (eV)	Trap concentration (cm^{-3})	Total trap concentration (cm^{-3})	Capture cross section (cm^2)	Introduction rate η (cm^{-1})	Recombination lifetime (s)	Effective lifetime (s)
9.4×10^{11}	ES21	A-center	$E_C - E_T = 0.163$	8.68×10^{13}	1.44×10^{14}	1.04×10^{-15}	92.6	1.64×10^{-6}	1.59×10^{-6}
	HS21	Di-vacancy	$E_V + E_T = 0.194$	1.70×10^{12}		4.00×10^{-16}	1.8	1.93×10^{-4}	
	ES22	A-center	$E_C - E_T = 0.218$	1.09×10^{12}		5.53×10^{-17}	1.2	1.94×10^{-3}	
	HS22	E-center	$E_V + E_T = 0.275$	7.59×10^{12}		3.54×10^{-17}	8.1	3.82×10^{-4}	
	ES23	D-center	$E_C - E_T = 0.533$	4.64×10^{13}		2.22×10^{-17}	49.5	8.35×10^{-5}	
3.1×10^{12}	ES11	A-center	$E_C - E_T = 0.160$	6.04×10^{13}	1.33×10^{15}	1.95×10^{-17}	19.3	1.28×10^{-4}	3.11×10^{-7}
	HS11	Di-vacancy	$E_V + E_T = 0.182$	1.08×10^{14}		5.06×10^{-17}	34.6	2.49×10^{-5}	
	ES12	$(B_i - O_i)$ complex	$E_C - E_T = 0.276$	1.67×10^{14}		5.18×10^{-17}	53.3	1.39×10^{-5}	
	ES13	Di-vacancy	$E_C - E_T = 0.385$	7.90×10^{13}		1.24×10^{-15}	25.3	1.04×10^{-6}	
	HS12	Si-interstitial	$E_V + E_T = 0.401$	1.40×10^{13}		1.54×10^{-17}	4.5	4.43×10^{-4}	
	ES14	D-center	$E_C - E_T = 0.557$	1.34×10^{14}		1.54×10^{-16}	42.9	4.20×10^{-6}	
	ES15	Defect cluster	$E_C - E_T = 0.581$	7.64×10^{14}		2.08×10^{-16}	244.4	5.26×10^{-7}	

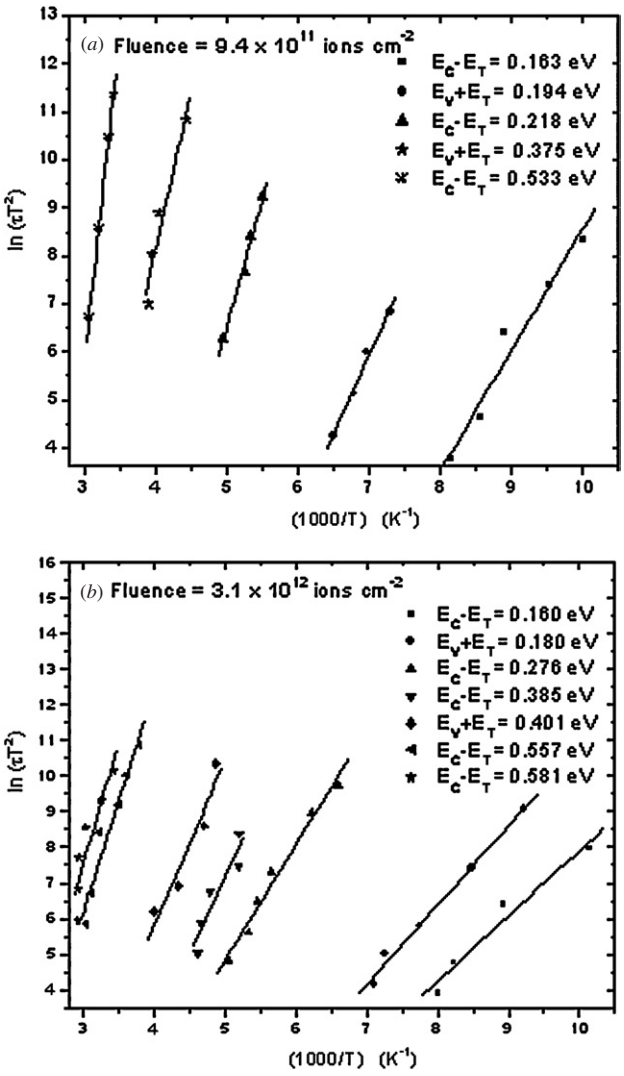

Figure 8. Arrhenius plots for ion fluences (*a*) 9.4×10^{11} ions cm^{-2}, (*b*) 3.1×10^{12} ions cm^{-2}.

In equation (3), B is the radiative recombination coefficient (for Si, $B \sim 10^{-14}$ cm^3 s^{-1}), p_0 is the equilibrium majority carrier concentration, n_0 is the equilibrium minority carrier concentration and Δn is the excess minority carrier concentration. The Auger recombination lifetime is given by

$$\tau_{\text{Auger}} = \left[c_p\left(p_0^2 + 2p_0\Delta n + \Delta n^2\right) + c_n\left(n_0^2 + 2n_0\Delta n + \Delta n^2\right)\right]^{-1}. \quad (4)$$

In equation (4), c_p and c_n are Auger recombination coefficients (for Si, c_p, $c_n \sim 10^{-31}$ cm^6 s^{-1}). Both Auger and radiative recombination can occur through intermediate (deep) levels, but are dominant only in direct band gap semiconductors [22]. These recombination mechanisms are utilized in light-emitting phosphors where semiconductors like CdS are deliberately doped with impurities of a particular kind to generate light of a particular wavelength.

Since the SRH recombination depends on trap concentration, it appears to be more predominant in our case. The values of SRH recombination lifetimes calculated using DLTS data and equation (2) are tabulated in table 2. The values of effective recombination lifetime and total trap concentration of observed deep level defects are also presented in table 2.

The transistor irradiated with fluence 3.1×10^{12} ions cm^{-2} is subjected for both isothermal and isochronal annealing, and the characteristics of each defect is monitored by recording the DLTS spectra. However, no significant changes are observed in the DLTS spectra as a function of annealing time at a given constant temperature (isothermal annealing). After isochronal annealing, significant changes are observed in the DLTS spectra. The total defect concentration decreases and the effective recombination lifetime increases with an increase in isochronal (30 min) annealing temperature, as shown in figure 9. A study of change in defect concentration with annealing temperature is useful in determining the type of defects. Figure 10 exhibits the variation of concentration of different deep level defects as a function of isochronal (30 min) annealing temperature. The annealing behavior of different deep level defects in silicon has been studied by several groups and documented well in the literature [28–32]. The identification of the defect type is made on the basis of their finger prints such as activation energy, annealing temperature and capture cross section by comparing with those reported in the literature.

$E_V + 0.182$ level. The introduction rate of the $E_V + 0.182$ level is 34.6 cm^{-1} and the capture cross section is 5.06×10^{-17} cm^2. This level anneals out at 300 °C–350 °C. Khan *et al* have

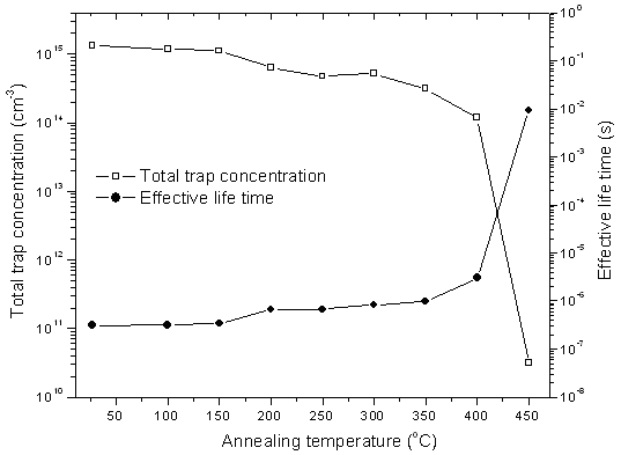

Figure 9. Variation of total trap concentration and effective lifetime as a function of isochronal (30 min) annealing temperature.

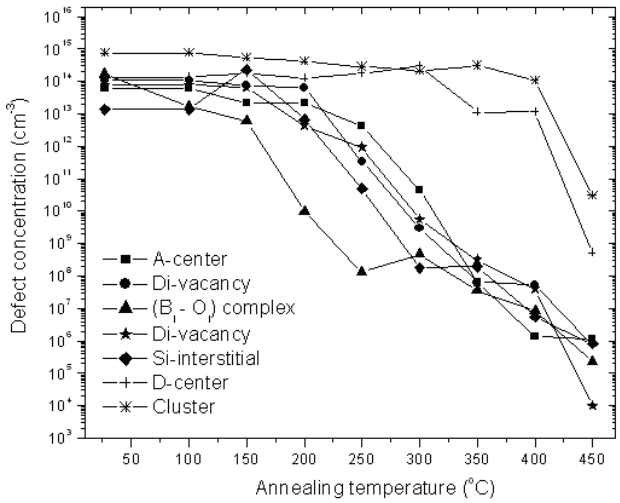

Figure 10. Variation of defect concentration as a function of isochronal (30 min) annealing temperature.

observed the $E_V + 0.180$ defect level in proton-irradiated silicon and assigned it to a di-vacancy which anneals out at 300–325 °C [33]. Based on the similarities in activation energy and annealing temperature, the $E_V + 0.182$ level could be attributed to a di-vacancy.

$E_C - 0.218$ level. The introduction rate of the $E_C - 0.218$ level is 1.2 cm^{-1} and the capture cross section is 5.53×10^{-17} cm^2. This level is observed to anneal out at 250 °C–300 °C. Gnana Prakash *et al* have identified the $E_C - 0.21$ level as an A-center with a capture cross section of 10^{-17} cm^2 [2]. Based on the similarities in activation energy and capture cross section, the $E_C - 0.218$ level could be assigned as an A-center.

$E_V + 0.275$ level. The introduction rate of the $E_V + 0.275$ level is 8.1 cm^{-1} and the capture cross section is 3.54×10^{-17} cm^2. This level anneals at 350 °C–400 °C. These signatures show that the $E_V + 0.275$ level is a new energy level for the E-center found by Larsen *et al* [34].

$E_C - 0.533$ and $E_C - 0.557$ levels. The introduction rates of $E_C - 0.533$ and $E_C - 0.557$ levels are 49.5 cm^{-1} and 42.9 cm^{-1}, respectively. The capture cross sections are 2.22×10^{-17} cm^2 and 1.54×10^{-16} cm^2. These levels appear to be stable even above 450 °C. These signatures resemble the properties of D-centers observed by Giri and Mohapatra [35, 36].

$E_C - 0.276$ level. The introduction rate of the $E_C - 0.276$ level is 53.3 cm^{-1} and the capture cross section is 5.18×10^{-17} cm^2. This level anneals out at 170 °C. Mooney *et al* have observed the defect $E_C - 0.27$ level in 1 MeV electron-irradiated silicon which anneals out at 170 °C [14]. Based on the dependence of the introduction rate of the $E_C - 0.27$ level on boron concentration, Mooney *et al* suggested that the $E_C - 0.27$ level is a defect complex formed by the trapping of interstitial boron by interstitial oxygen. Thus, the $E_C - 0.276$ level could be assigned to the boron–oxygen interstitial complex ($B_i - C_i$).

New defect levels. The introduction rates of the levels $E_C - 0.163$ and $E_C - 0.160$ are 92.6 cm^{-1} and 19.3 cm^{-1}, respectively. The capture cross sections are 1.04×10^{-15} cm^2 and 1.95×10^{-17} cm^2. These levels anneal out at 300 °C–350 °C. Brotherton and Bradley have observed A-center at $E_C - 0.169$ eV with a capture cross section of 10^{-14} cm^2. This level anneals out at 317 °C [12]. Benton *et al* have observed A-center at $E_C - 0.17$ eV in a Si-ion-implanted silicon sample. This level anneals out at 350 °C [37]. Based on these similarities, $E_C - 0.163$ and $E_C - 0.160$ levels observed in our study may be assigned as new energy levels for A-center.

Introduction rates of the levels $E_V + 0.194$ and $E_C - 0.385$ are 1.8 cm^{-1} and 25.3 cm^{-1}, respectively. The capture cross sections are 4×10^{-16} cm^2 and 1.24×10^{-15} cm^2. These levels anneal at 300 °C–400 °C. Walker and Sah have observed a di-vacancy at $E_V + 0.20$ eV which anneals out at 370 °C. Also, the production rate of this level is independent of boron concentration [30]. Mooney *et al* have suggested that the level $E_V + 0.20$ eV is a di-vacancy with a capture cross section of 10^{-16} cm^2, and it anneals out at 400 °C [14]. Benton *et al* have found a di-vacancy in a Si-ion-implanted silicon sample at $E_C - 0.40$ eV which anneals out at 400 °C [37]. Depending on these similarities, $E_V + 0.194$ and $E_C - 0.385$ levels may be assigned as new energy levels for di-vacancy.

The energy level $E_V + 0.401$ with the introduction rate 4.5 cm^{-1} and capture cross section 1.54×10^{-17} cm^2 anneals at 250 °C–300°C. Cherki and Kalma have concluded that the defects which give rise to energy levels located at $E_V + 0.395$ eV in aluminum-doped silicon as measured by infrared photoconductivity are dopant atoms in interstitial positions. This defect production is probable only where silicon interstitials are formed randomly by the irradiation. These defects are observed to anneal out at 250–300 °C [38]. Accordingly, the $E_V + 0.401$ level may be assigned as a new energy level for silicon interstitial.

Giri and Mohapatra have observed a level at $E_C - 0.56$ eV with a capture cross section 10^{-15} cm^2. This defect occurs in high-dose-irradiated samples and does not so prior to high-temperature annealing, suggesting that it is due to defect

clusters [36]. Thus, the level $E_C - 0.581$ observed in our study could be a new energy level for defect cluster with an introduction rate 244.4 cm^{-1} and capture cross section 2.08×10^{-16} cm^2 and is found to be stable even above 450 °C.

However, to identify the exact microscopic structure of these new defect levels, investigation by other structure-sensitive techniques such as electron paramagnetic resonance (EPR) and infrared photoconductivity measurements are required.

A comparison of *I–V* characteristics (figures 3 and 4) and DLTS results (figures 9 and 10) before and after annealing suggests that the defects which annihilate in the temperature range 350 °C to 450 °C have a major contribution to the change in the base and collector currents and hence degradation of the forward current gain of the transistor.

4. Conclusion

A commercial bipolar junction transistor (2 N 2219 A, npn) undergoes gain degradation upon irradiation by Si^{9+} ions due to displacement damage in the base region of the transistor. Deep level defects generated in the collector-base junction of the transistor are identified as electron traps with activation energies ranging from $E_C - 0.160$ eV to $E_C - 0.581$ eV and hole traps with activation energies from $E_V + 0.182$ eV to $E_V + 0.401$ eV. The identification of the defect type is made on the basis of their finger prints such as activation energy, annealing temperature and capture cross section by comparing with those reported in the literature. New energy levels for the defects A-center, di-vacancy and Si-interstitial are observed. DLTS studies after annealing show that the defects anneal above 350 °C. The defects generated in the base region of the transistor by displacement damage appear to be responsible for an increase in base current through SRH or multi-phonon recombination and consequent transistor gain degradation.

Acknowledgments

The authors thank Mr R N Dutt, Dr Safvan and Mr P Barua of IUAC, New Delhi, for their help during the experiments conducted at IUAC. One of the author (K V Madhu) thanks UGC-IUAC for a fellowship to carry out the present work. Financial support in the form of ISRO-RESPOND research project is acknowledged. The authors thank Dr V Pandian of M/s. Lab Equip. for many helpful discussions.

References

[1] Wei A, Kosier S L, Schrimpf R D, Fleetwood D M and Combs W E 1994 *Appl. Phys. Lett.* **65** 1918
[2] Gnana Prakash A P, Ke S C and Siddappa K 2004 *Semicond. Sci. Technol.* **19** 1029
[3] Summers G P, Wolicki E A, Xapsos M A, Marshall P, Dale C J, Gehlhauen M A and Olice R D 1986 *IEEE Trans. Nucl. Sci.* **NS-33** 1282
[4] Barnaby H J, Schrimpf R D, Sternberg A L, Berthe V, Cirba C R and Peace R L 2001 *IEEE Trans. Nucl. Sci.* **48** 2074
[5] Dale C J, Marshall P W, Burke E A, Summers G P and Wolicki E A 1988 *IEEE Trans. Nucl. Sci.* **35** 1208
[6] Lang D V 1974 *J. Appl. Phys.* **45** 3023
[7] Kulkarni S R, Sharma A, Joshi G R, Ravindra M and Damle R 2003 *Radiat. Eff. Defects Solids* **158** 647
[8] Kulkarni S R, Ravindra M, Joshi G R and Damle R 2004 *Radiat. Eff. Defects Solids* **159** 273
[9] Kulkarni S R, Ravindra M, Joshi G R and Damle R 2006 *Nucl. Instrum. Methods* B **251** 157
[10] Madhu K V, Kulkarni S R, Ravindra M and Damle R 2007 *Nucl. Instrum. Methods* B **254** 98
[11] Srour J R, Cheryl J M and Marshall P W 2003 *IEEE Trans. Nucl. Sci.* **50** 653
[12] Brotherton S D and Bradley P 1982 *J. Appl. Phys.* **53** 5720
[13] Srour J R, Long D M, Millward D G, Fitzwilson R L and Chadsey W L 1984 *Radiation Effects and Dose Enhancement of Electron Materials* (New Jersey: Noyes Publications)
[14] Mooney P M, Cheng L J, Suli M, Gerson J D and Corbett J W 1977 *Phys. Rev.* B **15** 3836
[15] Messenger S R, Burke E A, Xapsos M A, Summers G P, Walters R J, Jun I and Thomas Jordan R J 2003 *IEEE Trans. Nucl. Sci.* **50** 1919
[16] Jun I, Xapsos M A, Messenger S R, Burke E A, Walters R J, Summers G P and Jordan T 2003 *IEEE Trans. Nucl. Sci.* **50** 1924
[17] Jun I and McAlpine W 2001 *IEEE Trans. Nucl. Sci.* **48** 2034
[18] Summers G P, Burke E A, Shapiro P, Messenger S R and Walters R J 1993 *IEEE Trans. Nucl. Sci.* **40** 1372
[19] Harris R D, Frasca A J and Patton M O 2005 *IEEE Trans. Nucl. Sci.* **52** 2408
[20] Messenger S R, Burke E A, Summers G P and Walters R J 2002 *IEEE Trans. Nucl. Sci.* **49** 2690
[21] Messenger S R, Burke E A, Summers G P, Xapsos M A, Walters R J, Jackson E M and Weaver B D 1999 *IEEE Trans. Nucl. Sci.* **46** 1595
[22] Schroder D K 1990 *Semiconductor Material and Device Characterization* (NewYork: Wiley) pp 309, 361–2
[23] Watanabe K and Munakata C 1993 *Semicond. Sci. Technol.* **8** 230
[24] Pickel J C, Kalma A H, Hopkinson G R and Marshall C J 2003 *IEEE Trans. Nucl. Sci.* **50** 671
[25] Hangleiter A 1987 *Phys. Rev.* B **35** 9149
[26] Shockley W and Read W T 1952 *Phys. Rev.* **87** 835
[27] Khanna V K 2004 *Eur. J. Phys.* **25** 221
[28] Libertino S and Coffa S 2001 *Phys. Rev.* B **63** 195206–1
[29] Khan A, Yamaguchi M, Ohshita Y, Dharmarasu N, Araki K, Abe T, Itoh H, Ohshima T, Imaizumi M and Matsuda S 2001 *J. Appl. Phys.* **90** 1170
[30] Walker J W and Sah C T 1973 *Phys. Rev.* B **7** 4587
[31] Pellegrino P, Leveque P, Lalita J, Hallen A, Jagadish C and Svensson B G 2001 *Phys. Rev.* B **64** 195211–1
[32] Brotherton S D and Bradley P 1982 *J. Appl. Phys.* **53** 5720
[33] Khan A, Yamaguchi M, Hisamatsu T and Matsuda S 2000 *J. Appl. Phys.* **87** 2162
[34] Larsen A N, Mesli A, Nielsen K B, Nielsen H K, Dobaczewski L, Adey J, Jones R, Palmer D W, Briddon P R and Öberg S 2006 *Phys. Rev. Lett.* **97** 106402–1
[35] Giri P K and MohapatraY N 1997 *Appl. Phys. Lett.* **71** 1682
[36] Giri P K and MohapatraY N 1998 *J. Appl. Phys.* **84** 1901
[37] Benton J L, Libertino S, Kringhoj P, Eaglesham D J, Coffa S and Poate J M 1997 *J. Appl. Phys.* **82** 120
[38] Cherki M and Kalma A H 1970 *Phys. Rev.* B **1** 640